Resonant inelastic scattering of an x-ray photon by the argon atom near K and KM_{23} ionization thresholds

Alexey Hopersky,* Alexey Nadolinsky, and Victor Yavna
Chair of Mathematics, Rostov State University of Transport Communication, Rostov-on-Don, 344038, Russia
(Received 3 November 2006; revised manuscript received 15 December 2006; published 30 January 2007)

The influence of many-particle effects on the absolute values and the shape of doubly differential cross section of resonance inelastic scattering of a linearly polarized x-ray photon by the free Ar atom near K and KM_{23} ionization thresholds is studied theoretically. Shown is the evolution of spatially extended profile of the scattering cross section into the principal $K\beta_{1,3}$ and satellite $K\beta^V$ structures of the Ar $K\beta$ emission spectrum. The calculations are performed in nonrelativistic Hartree-Fock approximation for the atomic wave functions and in the dipole approximation for the anomalous-dispersion scattering amplitude. The following many-particle effects are included: radial relaxation of electron shells, correlational loosening, vacuum correlations, spin-orbital, and multiplet splitting, configuration interaction in doubly excited atomic states, Auger and radiative decays for the vacancies produced. Calculations results are predictions while for the case of the incident photon energies of 3199.2 and 3245.9 eV they compare well with the results of the synchrotron experiment of Deslattes *et al.* [Phys. Rev. A **27**, 923 (1983)] on measuring the x-ray $K\beta$ emission spectrum of the free Ar atom.

DOI: 10.1103/PhysRevA.75.012719 PACS number(s): 32.80.−t, 32.30.Rj, 31.30.Jv

I. INTRODUCTION

Theoretical and experimental studies of photon-excited x-ray emission spectra of *free* atoms allow one to obtain fundamental information on the nature, the role, and the quantum interference of many particle effects in the processes of inelastic scattering of photon by an atom.

Deslattes *et al.* [1] were the first to perform the synchrotron experiment on measuring the x-ray $K\beta$ emission spectrum of the free Ar atom ($Z=18$, ground state configuration $[0]=1s^22s^22p^63s^23p^6[^1S_0]$) in the energy region of K, KM_1, and KM_{23} ionization thresholds. Principal spectral feature were assigned. Tulkki [2] performed the first theoretical calculation of the cross section of inelastic scattering of photon by the free Ar atom and demonstrated the evolution of the cross section into the $K\beta_{1,3}$ structure of the emission spectrum. The role of many particle effects in the formation of the emission spectrum has not been considered in Refs. [1,2].

In this work we report on the first theoretical study of the role of a wide hierarchy of many particle effects in the process of resonant inelastic (Landsberg and Mandelstam [3], Raman [4], Compton [5], see also reviews by Åberg and Tulkki [6] and Kane [7]) scattering of an x-ray photon in the energy region of K and KM_{23} ionization thresholds of the free Ar atom.

Experimental studies of photon-excited x-ray emission spectra of free atoms near their inner-shell ionization thresholds are scarce. Except the work [1] we know only the works by Raboud *et al.* [8] (Ar $K\alpha$ spectra), Czerwinski *et al.* [9] (Xe $K\alpha,\beta$ spectra) and MacDonald *et al.* [10] (Xe $L\alpha,\beta$ spectra).

One may suppose that the realization of the project of creation of the x-ray free electron laser (XFEL) with tunable wavelengths λ from 60 to 1.0 Å (incident photon energy from 0.2 to 12.4 keV) (Kornberg *et al.* [11]) will provide the opportunity of further experimental investigation of extended-in-space (three-dimensional: cross section, incident photon energy $\hbar\omega_1$, scattered photon energy $\hbar\omega_2$; $\omega_{1,2}$ is the photon cyclic frequency, $\hbar$ is the Planc constant) resonant structures of photon scattering cross sections near inner-shell ionization thresholds of free atoms.

At the same time, experimental and theoretical studies of the role of the many particle effects in the process of resonant inelastic scattering of the soft and the hard (incident photon energy from 300 eV to 1.5 MeV) x rays in the energy regions of inner-shell ionization thresholds of free atoms is in great demand in modern physics.

Particularly, they are important in the context of creation, together with the XFEL, of an laboratory-plasma x-ray laser generating with the participation of the deep $1s$ shell in lighter ($Z\leq 20$) atoms (Daido [12]), in laser thermonuclear fusion (generation and control of directed-to-target $K\alpha,\beta$ radiation (Lindl [13])), in observation and assignment of astrophysically significant Ar $K\alpha,\beta$ emission spectrum (Miceli *et al.* [14]), and in theoretical description of resonant inelastic scattering of an x-ray photon by such many-electron systems as atoms, ions, molecules (Gel'mukhanov and Ågren [15]), and simple clusters (Kotani and Shin [16]).

II. THEORY

Let us derive the analytical structure of doubly differential cross section of the process under study in standard second-order quantum-mechanical perturbation theory.

Consider a known structure of the nonrelativistic operator of the interaction of the electromagnetic field with an atom in Coulombic calibration for the field

$$\hat{Q}=\frac{e}{m_e c}\sum_{i=1}^{N}\left[\frac{e}{2c}(\mathbf{A}_i\cdot\mathbf{A}_i)-(\mathbf{p}_i\cdot\mathbf{A}_i)\right],$$

*Corresponding author. Email address: hopersky_vm_1@rgups.ru

$$\mathbf{A}_i \equiv \mathbf{A}(\mathbf{r}_i,0), \tag{1}$$

where c is the speed of light, e is electron charge, m_e is electron mass, N is the number of electrons in an atom, $\mathbf{A}$ is the operator (in secondary quantization representation) of the electromagnetic field at the time $t=0$, $\mathbf{p}_i$ is the momentum operator, and $\mathbf{r}_i$ is the position vector of the ith atomic electron.

The first sum in the operator $\hat{Q}$ from Eq. (1) determines the analytical structure of the probability amplitude for the so called *contact* [7,16] scattering of photon by an atom. In this case, in the representation of Goldstone-Hubbard-Feynman diagrams of the nonrelativistic quantum many-body theory, four line meet in the node of interaction of the electromagnetic field with an atom: two photon lines $(\hbar\omega_1, \hbar\omega_2)$, vacancy line, and the line of the excited electron. This amplitude is not the subject of this study, we shell mention the contribution of the contact scattering to the total doubly differential cross section of scattering of photon by the Ar atom only during the discussion of the results obtained.

The second sum in the operator $\hat{Q}$ from Eq. (1) determines the analytical structure of the *anomalously-dispersive* part of the probability amplitude for the resonant inelastic scattering of photon by an atom. In this case, the scattering amplitude in the representation of Goldstone-Hubbard-Feynman diagrams has a node with three lines: photon line, $\hbar\omega_1(\hbar\omega_2)$, vacancy line and excited electron (vacancy) line. It is the matrix element of this sum that we study in this work.

Consider the process of resonant inelastic scattering of the linearly polarized x-ray photon in the energy region of the Ar K ionization threshold of the type (hereafter the closed shells are omitted in configurations notations)

$$\hbar\omega_1 + [0] \to 1snp(^1P_1) \to 3p^5mp(^1S_0, {}^1D_2) + \hbar\omega_2, (n,m)p > f, \tag{2}$$

in the case of the scheme of the synchrotron experiment by Deslattes *et al.* [1], $\mathbf{e}_{1,2} \perp P$. Here f is the Fermi level (the set of the quantum numbers of the atomic valence shell), polarization vectors of incident $(\mathbf{e}_1)$ and scattered $(\mathbf{e}_2)$ photons, and the scattering plane P, containing the wave vectors of incident and scattered photons.

Note that the sequence of the transitions from Eq. (2) with the $^1P_1$ final-state term is forbidden by the Eckart-Wigner theorem: for the $1snp(^1P_1) \to 3p^5mp(^1P_1)$ emission transition there appears the $3j$ - Wigner coefficient

$$\begin{pmatrix} 1 & 1 & 1 \\ 0 & 0 & 0 \end{pmatrix} = 0.$$

We do not include intermediate $(2s,3s)np$ and $(2p^5,3p^5)n(s,d)$ scattering states since the threshold energies for the shells $nl \neq 1s$ in the Ar atom are well separated from the $1s$ threshold. For example, $I_{1s} - I_{2s} \cong 2.88$ keV (experimental data of Deslattes *et al.* [17]).

Then $(\mathbf{e}_1 \cdot \mathbf{e}_2)^2 = 1$, and the known general analytical expression for the anomalously-dispersive part of doubly differential cross section of resonance inelastic scattering of photon by an atom (Kramers-Heisenberg-Waller formula) [6], after summation (integration) over one-electron np intermediate and mp final scattering states of discrete (continuous) spectra and summation over the $^1S_0$ and $^1D_2$ terms, has the form (in atomic units, $e=\hbar=m_e=1$)

$$\frac{d^2\sigma_\perp}{d\omega_2 d\Omega} = r_0^2\left(\frac{\omega_2}{\omega_1}\right)\eta\alpha_{1s}g^{-1}\sum_{i=1,2}\zeta_i(R_i + C_i), \tag{3}$$

$$R_i = \sum_{n>f}^{\infty} A_n^2 L(\omega_1, I_n) G(\omega_{12}, I_n^i), \tag{4}$$

$$C_i = \left(1 + \frac{\omega_{12}}{I_{1s}}\right)^2 L(\omega_2, I_{1s} - I_{3p}^i) J_i, \tag{5}$$

$$J_i = \int_0^\infty A_\varepsilon^2 G(\varepsilon, \omega_{12} - I_{3p}^i) d\varepsilon. \tag{6}$$

The sum over the transitions into the discrete spectrum states in Eq. (4) gives the description of resonant Landsberg-Mandelstam-Raman scattering of photon by an atom. Expression (5) describes resonant Compton scattering (final state of the scattering is the continuous spectrum state) of photon by an atom.

In Eqs. (4) and (6), determined is the radial part of the probability amplitude for the radiative transition

$$A_n = \langle 1s_0 | \hat{r} | np_c \rangle, \tag{7}$$

from initial to intermediate scattering state of discrete (n)/continuous (ε) spectrum described by the correlation wave function

$$|np_c\rangle = N_s\left(|np_+\rangle - \sum_{k=2,3} |kp_+\rangle \frac{\langle kp_0 | np_+ \rangle}{\langle kp_0 | kp_+ \rangle}\right), \tag{8}$$

$$N_s = \langle 1s_0 | 1s_+ \rangle \langle 2s_0 | 2s_+ \rangle^2 \langle 2p_0 | 2p_+ \rangle^6 \langle 3s_0 | 3s_+ \rangle^2 \langle 3p_0 | 3p_+ \rangle^6, \tag{9}$$

$$\langle 1s_0 | \hat{r} | np_+ \rangle = \int_0^\infty P_{1s_0}(r) P_{np_+}(r) r dr, \tag{10}$$

$$\langle kp_0 | np_+ \rangle = \int_0^\infty P_{kp_0}(r) P_{np_+}(r) dr, \tag{11}$$

where, for example, $P_{np_+}(r)$ is the radial part of the np_+ electron wave function.

Analytical structure of the correlational wave function from Eqs. (8)–(11) is determined by the methods of the theory of nonorthogonal orbitals (Jucys *et al.* [18]) and expressed through nonrelativistic wave functions of one-electron states optimized in different Hartree-Fock fields. At that, significant is (von Zülicke [19], Sukhorukov *et al.* [20]) the demand of the orthogonality of the wave function of the $1s \to (n,\varepsilon)p$ excitation/ionization state to the wave functions of lower-lying $(2s,3s) \to (n,\varepsilon)p$ excitation/ionization states of the same symmetry. This demand is fulfilled in this work

using the Gram-Schmidt algorithm (Reed and Simon [21]) which is widely used in functional analysis. Resulting, the terms $\langle 1s_0|ks_+\rangle\langle ks_0|\hat{r}|np_+\rangle/\langle ks_0|ks_+\rangle$, $k=2,3$ are absent in Eq. (7).

The appearance of the deep $1s$ vacancy in atomic core leads, in the first place, to significant decrease of the outer core shells mean radius. The displacement of the atomic residue electron density towards the nucleus is accompanied by the delocalization of the np electron wave function. This many-particle effect is known as the effect of radial relaxation of one-electron states' wave functions upon appearance of a deep vacancy (Sukhorukov *et al.* [22], Amusia [23], Schmidt [24]).

In the problem we solve here, the influence of radial relaxation effect on the amplitude A_n from Eq. (7) is included as follows. The radial parts of the l_+ electrons' wave functions are obtained by the solution of nonlinear integrodifferential self-consistent field Hartree-Fock system of equations for the intermediate scattering state configuration $1snp(^1P_1)$ (in the field of the $1s$ vacancy). The radial parts of the l_0 electrons' wave functions are optimized for initial state of scattering [0].

For the radial overlap integrals for the wave functions of excited electrons in intermediate $(np_+,\varepsilon p_+)$ and final $(mp,\varepsilon' p)$ states the following approximation is used:

$$\langle np_+|mp\rangle \to \delta_{nm}, \quad \langle np_+|\varepsilon' p\rangle \to 0, \quad \langle \varepsilon p_+|mp\rangle \to 0, \tag{12}$$

where δ_{nm} is the Kronecker-Weierstrass symbol.

Hopersky *et al.* [25] went outside the frame of the approximation from Eq. (12) in their study of photon-excited of the free Ne atom x-ray $K\alpha$ emission spectrum at the energies near K and KL_{23} ionization thresholds and called this the inclusion of the many-particle effect of *correlational amplitudes*.

This effect is important outside the regions of formation of scattering spectrum resonant structures. It is, therefore, possible to neglect the effect of correlational amplitudes in the calculation of absolute values and profiles of the leading scattering spectrum resonance structures. Inclusion of this effect will be the subject of our further studies.

In addition, we use the approximation

$$\langle \varepsilon p_+|\varepsilon' p\rangle \to \delta(\varepsilon-\varepsilon'), \tag{13}$$

where δ is the generalized Dirac function. It follows then that we neglect the effect of the post collision interaction (PCI) (see Refs. [23,24]). In our case the effect of the PCI is the effect of modification of the radial part of photoelectron continuous spectrum wave function due to the radiation $1s \to 3p^5+\hbar\omega_2$ decay of the deep $1s$ vacancy.

Hopersky [26,27] and Hopersky and Chuvenkov [28] showed that the inclusion of the PCI effect [modification of photoelectron continuous spectrum wave function due to the radiationless $1s \to 2p^4\varepsilon d$ Auger decay of the $1s$ vacancy and go out the frame of Eq. (13)] in theoretical K photoabsorption spectra of light ($Z \leq 20$) atoms practically not leads to any changes of the results in comparison with the ones in one-electron approximation. One may suppose that the PCI effect upon radiative $1s \to 3p^5+\hbar\omega_2$ decay of the $1s$ vacancy will not change the one-electron-approximation results. However, additional studies are needed to state it rigorously.

In Eqs. (3)–(6), L is the Cauchy-Lorentz and G is the Gaussian instrumental (experimentally taken function of the distribution of the radiation incident on atom) functions

$$L(x,y) = \frac{\gamma_{1s}}{\pi}\frac{1}{(x-y)^2+\gamma_{1s}^2}, \tag{14}$$

$$G(x,y) = \frac{1}{\gamma_b\sqrt{2\pi}}\exp\left\{-\left(\frac{x-y}{\gamma_b\sqrt{2}}\right)^2\right\}. \tag{15}$$

Also the following notations are introduced: r_0 is the electron classical radius, Ω is the solid angle of scattered photon escape, g is the statistical weight of the intermediate scattering state, $\alpha_{1s}=\alpha\pi I_{1s}^4/\gamma_{1s}$, α is a resulting angular transition coefficient (product of the angular parts of the probability amplitudes for the transitions from initial to intermediate and from intermediate to final scattering states), $\gamma_{1s}=\Gamma_{1s}/2$, Γ_{1s} is the total (over the channels of radiative and Auger type) $1s$ vacancy decay width (natural width of the x-ray K level), $\gamma_b=\Gamma_{beam}/2$, Γ_{beam} is the parameter of the instrumental Gaussian function, $\zeta_i=\{2,i=1;1,i=2\}$; I_n is the energy of $1s \to np$ excitation, $I_n^i=\{I_{3pnp},i=1;I_{3pnp}+\delta_{SO},i=2\}$, I_{3pnp} is the energy of $3p \to np$ excitation, δ_{SO} is the spin-orbit split constant of the valence $3p_{1/2,3/2}$ shell; $I_{3p}^i=\{I_{3p},i=1;I_{3p}+\delta_{SO},i=2\}$, $I_{1s(3p)}$ is the $1s(3p)$ shell threshold ionization energy, $\omega_{12}\equiv\omega_1-\omega_2$.

Note that due to a limited lifetime ($\tau_{1s}=\hbar\Gamma_{1s}^{-1}$) $1s$ state is *metastable* and it does not survive in the process of scattering. This fact is analytically expressed by the appearance in Eqs. (3)–(6) of the spectral function of density of excited intermediate scattering states of the Cauchy-Lorentz type $L(\omega_1-I_{1s},x)$ from Eq. (14), where x is the energy of the excited from the $1s$ shell one-electron $(n,\varepsilon)p$ state.

In Eq. (3) the quantity $\sqrt{\eta}$ is determined as the radial part of the probability amplitude for the radiative transition from intermediate to final scattering state

$$\sqrt{\eta} = \langle 1s|\hat{r}|3p_c\rangle, \tag{16}$$

$$|3p_c\rangle = N_{sp}\left(|3p_+\rangle - |2p_+\rangle\frac{\langle 2p|3p_+\rangle}{\langle 2p|2p_+\rangle}\right), \tag{17}$$

$$N_{sp} = \langle 1s|1s_+\rangle\langle 2s|2s_+\rangle^2\langle 2p|2p_+\rangle^6\langle 3s|3s_+\rangle^2\langle 3p|3p_+\rangle^5. \tag{18}$$

In Eqs. (16)–(18) the radial parts of the l electrons' wave functions are obtained by the solution of the averaged over $^1S_0$ and $^1D_2$ terms Hartree-Fock equations for the final-scattering state configuration $3p^5np$ (in the field of the valence $3p$ vacancy).

The amplitudes A_n from Eq. (7) and $\sqrt{\eta}$ from Eq. (16) are determined in *dipole* approximation for the Fourier-components of the electromagnetic field operator $\mathbf{A}_j$ in the second sum of the operator $\hat{Q}$ from Eq. (1)

$$(\mathbf{k}\cdot\mathbf{r}_j)\to 0 \Rightarrow \exp\{i(\mathbf{k}\cdot\mathbf{r}_j)\}\to 1, \quad i^2=-1, \tag{19}$$

where $\mathbf{k}$ is the wave vector of incident (scattered) photon, $\mathbf{r}_j$ is the position vector of the atomic jth electron.

It is known [7] that the dipole approximation from Eq. (19) is equivalent to the fulfillment of the relation

$$\lambda \gg r_{nl}, \tag{20}$$

where λ is the wavelength of incident (scattered) photon, and r_{nl} is the mean radius of the nl shell determining the radial integral of radiative transition (in our case, $nl=1s$). For the x-ray energy regions studied in this work the relation (20) is fulfilled. Indeed, for the energies incident photon ω_1 from 3195 to 3250 eV (λ from 3.883 to 3.817 Å) and scattered photon ω_2 from 3180 to 3215 eV (λ from 3.901 to 3.859 Å) we have $\lambda \gg r_{1s}$ (Ar)=0.046 Å. Here we used the relation

$$\lambda[\text{Å}] = \frac{12406.764}{\omega[eV]}.$$

Radial integrals in the amplitudes A_n from Eq. (7) and $\sqrt{\eta}$ from Eq. (16) are calculated in the length form for the transition operator. Our study showed that the use of the velocity form for the transition operator in the calculation of integrals with the deep $1s$ shell in atoms with $Z\geq 10$ changes the amplitudes by not more than $\sim 1\%$. It follows then that the effect of the correlations of random phase approximation with exchange (Amusia [23]) [in the case of Ar, electrostatic mixing of the configuration $1snp$ with virtual ionization configurations $ks\varepsilon p$ and $kp^5\varepsilon(d,s)$ $(k=2,3)$ as inclusion of intershell correlations] is insignificant, and it was not considered in this work.

Together with the radial relaxation effect, we include also the next-order effects in the analytical structure of the scattering probability amplitude. Specifically, we include the many-particle effects of *correlational loosening* (CL), *vacuum correlations* (VC), and double excitation/ionization of the atomic ground state.

Physical nature and influence of the CL and VC effects on absolute values and profile of the photoabsorption cross section in the energy region of the Ar K ionization threshold are studied by Hopersky and Yavna [29]. Sukhorukov *et al.* [30] studied the absolute values and profile of the photoabsorption cross section near K, KM_1, and KM_{23} ionization thresholds of the Ar atom.

The analytical structure of the amplitude of the resonant inelastic scattering with inclusion of double excitation/ionization effects in the Ar atom ground state will be presented in the discussion of the results. Here we give a short description of the CL and VC effects [29].

The CL and VC effects are due to virtual excitations/ionization in initial and final photoabsorption states. Thus in many-configuration approximation the wave functions of initial $|\bar{0}\rangle$ and final $|\omega\rangle$ (in the case of scattering, intermediate) K photoabsorption states may be presented as follows (let us limit ourselves to with the case of np photoelectron in discrete spectrum)

$$|\bar{0}\rangle = \alpha_0\left(|0\rangle + \int_0^\infty\int_0^\infty \beta_{xy}|xy\rangle dxdy\right), \tag{21}$$

$$|\omega\rangle = \alpha_{\omega n}\left(|1snp\rangle + \sum_{m_{1,2}>f}^{\infty}\rho_{12}^{\omega}|m_1m_2n\rangle + \int_0^\infty \chi_n^{\omega}(\varepsilon)|n\varepsilon\rangle d\varepsilon\right), \tag{22}$$

$$\langle\bar{0}|\bar{0}\rangle = 1, \quad \langle\omega|\omega'\rangle = \delta(\omega-\omega'), \tag{23}$$

$$|\alpha_{\omega n}|^2 = L(\omega, I_n). \tag{24}$$

Here $|0\rangle$ and $|1snp\rangle$ are initial and final photoabsorption states in one-configuration approximation, $|n\varepsilon\rangle$ is the wave function of the configuration for the principal $1s$ vacancy Auger $1snp\to(2p^4\varepsilon d)np$ decay channel, α_0 is a normalizing factor, β, ρ, χ are the configuration mixing coefficients, ω is the absorbed photon energy.

The principal contribution ($\sim 80\%$) in the structure of the wave function from Eqs. (21) and (23) is from the channels of double ionization of the [0]-*Fermi-vacuum* $3p$ subshell into the states of p and d symmetry: $|xy\rangle \to |3p^4x(p,d)y(p,d)\rangle$.

The principal contribution ($\sim 85\%$) in the structure of the wave function from Eqs. (22)–(24) is from the channel of double excitation of valence $3p$ subshell into the d symmetry states: $|m_1m_2n\rangle\to|1s(3p^4m_1dm_2d)np\rangle$.

It follows from Eqs. (21) and (22) that in the total K photoabsorption amplitude, the leading radiation $1s\to np$ transition amplitude interferes with radiation transitions amplitudes $|0\rangle\to|m_1m_2n\rangle$, $|0\rangle\to|n\varepsilon\rangle$, $|xy\rangle\to|1snp\rangle$, $|xy\rangle\to|n\varepsilon\rangle$, and $|xy\rangle\to|m_1m_2n\rangle$. Inclusion of this interference in the calculation of the absolute values and the shape of the ArK photoabsorption cross section is considered in Ref. [29] as inclusion of the VC effect. For example, VC effect increases the probability of $1s\to 4p$ transition in the Ar atom by $\sim 12\%$ as compared with a one-electron calculation.

"Loosening" of the valence $3p$ subshell of the atomic residue by double excitations $3p3p\to m_1dm_2d$ causes the np photoelectron to move in the Hartree-Fock field of the configuration

$$1s3p^{N_1}3d^{N_2}np \tag{25}$$

with *effective* occupancy numbers of the core $3p$ and excited $3d$ subshells

$$N_1 = 6-N_2, \quad N_2 = 2(1-s), \tag{26}$$

$$s = \left(1+\sum_{m_{1,2}>f}^{\infty}|\rho_{12}^{\omega}|^2\right)^{-1}, \tag{27}$$

where s is the spectroscopic factor (see Ref. [23]) of the $1snp$ state.

In configuration (25), a nonzero occupancy numbers of excited $m_{1,2}d$ orbitals is presented only by the $3d$ subshell electron density since double $3p3p\to 3d3d$ excitation gives the principal contribution ($\sim 65\%$) to s from Eq. (27).

TABLE I. Absolute values of doubly differential LMRS cross section from Eq. (41) near the KM_{23} ionization threshold of the free Ar atom (see Fig. 3).

n[a]	$\hbar\omega_{1n}$[b] (eV)	$\sigma_\perp$[c]
1	3223.5	57.00
2	3223.6	60.07
3	3224.4	86.88
4	3224.7	60.01
5	3225.6	16.74
6	3226.6	36.22

[a]$|n\rangle$ is are intermediate scattering states, see Eq. (33).
[b]$\hbar\omega_{1n}$ is the incident photon energy, see Eq. (34). Emission photon energy is $\hbar\omega_0$=3193.3 eV [see Eq. (35)].
[c]$\sigma_\perp \equiv d^2\sigma_\perp/d\hbar\omega_2 d\Omega$ in units of r_0^2 eV^{-1} sr^{-1}, r_0^2=7.941 $\times 10^{-26}$ cm^2.

The switching in expression (25) from N_1=6 and N_2=0 to N_1=5.8 and N_2=0.2 from Eqs. (26) and (27) in Hartree-Fock equations changes the solution for the radial part of the np photoelectron wave function. For example, this leads to about 5% increase of the $1s \rightarrow 4p$ transition probability in the Ar atom as compared with a one-electron value. In Ref. [29] this is described as the CL effect. One should note that the effective occupancy numbers method as a practical alternative to the solution of many-configuration self-consistent field Hartree-Fock-Jucys equations (Jucys [31], Froese-Fischer [32]) goes back to early work by Kulagin and Zalyubovski [33].

III. RESULTS AND DISCUSSION

We study a free Ar atom. Calculated doubly differential cross section of resonant scattering of an x-ray photon by the Ar atom in the energy regions of incident ω_1 from 3195 to 3250 eV and scattered ω_2 from 3175 to 3215 eV photons are presented in Tables I and II and Figs. 1–4.

The following values of the total nl vacancy decay widths (Γ_{nl}) are used: Γ_{1s}=0.690 eV (experiment by Morgan *et al.* [34]), Γ_{2s}=2.330 eV (experiment by Kylli *et al.* [35]), Γ_{2p} =0.115 eV (theoretical value by Gorczyca and Robicheaux [36]), $\Gamma_{3s}=1.41\times10^{-7}$ eV, and $\Gamma_{3p}=1.74\times10^{-17}$ eV. The two latter values are obtained from the formula

$$\Gamma_{nl}[\mathrm{eV}] = \frac{6.586}{\tau_{nl}[s]} \times 10^{-16},$$

where the lifetimes for $3s$ and $3p$ vacancies are measured by Lauer *et al.* [37] ($\tau_{3s}=4.684\times10^{-9}$ s) and Katori and Shimizu [38] (τ_{3p}=37.88 s). The parameter of the Gaussian function from Eq. (15) is taken to be Γ_{beam}=1.30 eV (instrumental resolution of the work of Deslattes *et al.* [1]). Theoretical value δ_{SO}=0.179 eV of constant of the spin-orbit split of the $3p_{1/2,3/2}$ shell is from the work of Huang *et al.* [39].

The following values of the ionization thresholds energies (I_{nl}) of the core nl subshells are used I_{1s}=3206.26 eV (experiment by Breinig *et al.* [40]), I_{2s}=326.25 eV (experiment by Glans *et al.* [41]), I_{2p}(eV)=248.46(L_3); 250.57(L_2) (experimental data from Deslattes *et al.* [17]), and I_{nl}(eV) =29.24($3s$); 15.76 ($3p,M_3$); 15.94 ($3p,M_2$) (experimental data from Karazija [42]).

TABLE II. Intermediate state $\zeta(T_1)np(T_2)\varepsilon' p$ and final state $3p^4(T_3)np(T_4)\varepsilon' p$ wave functions of resonance inelastic scattering of linearly polarized (perpendicularly to the scattering plane) x-ray photon near KM_{23} ionization threshold of the free Ar atom.

n	T_1	T_2	T_3	T_4	$\hbar\omega_2$ (eV)[a]	N[b]	$\sigma_\perp$[b]
4	ψ_1[c]	^1S	^2P	3191.25		0.82
	^2D	^2D	^1D	^2F	3192.85		2.41
	^2D	^2P	^1D	^2D	3193.10		0.79
	ψ_1		φ_1[c]	3193.25	1	4.04
	^3P	^2D	φ_3	3193.35		1.18
	^3P	^2D	^3P	^2D	3193.55	3	4.06
	ψ_3		^3P	^2S	3193.70		1.42
	ψ_3			φ_3	3193.71		0.82
	^3P	^2S		φ_3	3193.75	4	3.42
	ψ_3		^3P	^2D	3193.90		1.80
5	ϕ_1[c]	^1D	^2P	3193.30		1.75
	^3P	^2D	^3P	^2D	3194.00		1.35
ε	^2D	$^2(S,P,D)$	^1S	^2P	3191.25		0.75
	^2D	$^2(S,P,D)$	^1D	$^2(P,D,F)$	3193.45	2	3.61
	^3P	$^2(S,P,D)$	^3P	$^2(S,P,D)$	3194.20	5	5.86

[a]Energy at which respective spatially extended structure of the cross sections from Eqs. (50) and (57) appears [see Figs. 3 and 4(b)]. Absorbed photon energy is $\hbar\omega_1$=3245.9 eV.
[b]N is the resonance number and $\sigma_\perp \equiv d^2\sigma_\perp/d\hbar\omega_2 d\Omega$ is the absolute values (in units of r_0^2 eV^{-1} sr^{-1}, $r_0^2=7.941\times10^{-26}$ cm^2) of the cross sections from Eqs. (50) and (57) in Fig. 4(b) for the x-ray satellite $K\beta^V$ emission spectrum of the Ar atom.
[c]ψ_i –, ϕ_i –, φ_i — see Eqs. (46)–(48).

A. K ionization threshold energy range

Doubly differential cross section from Eq. (3) near the Ar K ionization threshold is presented in Fig. 1.

The wave functions [see Eqs. (21) and (22)], and the energies of initial and intermediate states are obtained in many-configuration Hartree-Fock approximation [for the np photoelectron wave function of the intermediate state — in the field of the configuration from Eq. (25)]. Final-scattering-state wave functions and energies are obtained in one-configuration Hartree-Fock approximation.

Included are the one-electron np intermediate and mp final scattering states with n,m=4,5,6, which form the leading resonances of scattering at photon energies (in eV) of (ω_1,ω_2)=(3203.66;3190.24), (3205.02; 3190.26), (3205.53; 3190.30).

We did not study the problem of completeness of the discrete states set (n,m=4 to ∞) in this work. Hopersky *et al.* studied this problem analytically in the cases of anomalous *elastic* scattering of an x-ray photon by the Ne atom and the

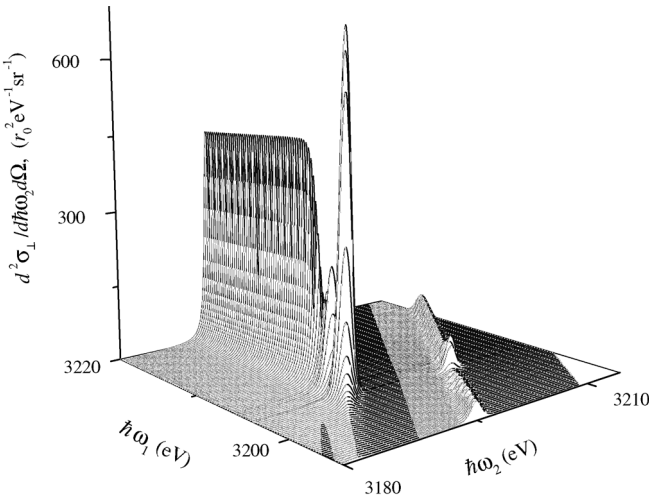

FIG. 1. Doubly differential cross section of inelastic scattering of linearly polarized (perpendicularly to the scattering plane) x-ray photon near K (3206.26 eV, from Ref. [40]) ionization threshold of the free Ar atom. $\hbar\omega_1(\hbar\omega_2)$ are the energies of incident (scattered) photon. Ω is a solid angle of escaping scattered photon, Γ_{beam} =1.30 eV (from Ref. [1]), Γ_{1s}=0.69 eV (from Ref. [34]), δ_{SO} =0.179 eV (from Ref. [39]). Spatially extended structure of the cross section at $\hbar\omega_2=\hbar\omega_1$ corresponds to the elastic scattering at θ=90° (see Fig. 2).

multiply charged positive ions Ne^{6+}, Si^{4+}, and Ar^{8+} in Refs. [43,44]. Generalization of the results obtained in Refs. [43,44] for the case of resonant *inelastic* scattering of an x-ray photon near inner-shell ionization thresholds of the atoms and ions will be the subject of our further investigations.

According to the resonance condition of the Compton profile C_i from Eq. (5), the continuous spectrum channels $3p^5\varepsilon_i p$ are opened at $\omega_1=I_{1s}$ and $\omega_2=I_{1s}-I^i_{3p}$=3190.32 (M_2); 3190.50 (M_3) eV. At $\omega_1>I_{1s}$ the cross section from Eq. (3) attains a spatially extended profile of the x-ray Ar $K\beta_{1,3}$ emission spectrum.

Inclusion of the effect of radial relaxation of the intermediate states electron shells in the field of the deep 1s vacancy leads to almost two-fold decrease of the absolute values of the cross section from Eq. (3) as compared with the results obtained neglecting this effect. Topologically, the no-radial-relaxation cross section is the same as the one obtained with the relaxation effect included; it is not shown in Fig. 1.

Inclusion of the CL(VC) effect increases by 5(12)% (1s $\rightarrow 4p$ transition), 3(7)% (1$s\rightarrow 5p$ transition), 1(2)% (1s $\rightarrow 6p$ transition), and 5(20)% (1$s\rightarrow\varepsilon p$transition near the K threshold) the cross sections calculated with inclusion of only the radial relaxation effect.

Riblike structures going at the angle of 45° in the plane $(\omega_1;\omega_2)$ to the both sides of each resonance and from the threshold of the $K\beta_{1,3}$ scattering spectrum structure are due to the presence in Eq. (3) of spectral $G(\omega_{12},I^i_n)$ Gaussian functions (power of the exponent is zero on the lines ω_1 $=\omega_2+I^i_n$) and minimal, ε_i=0, energy of the continuous spectrum electron (probability amplitude for the radiative transition A_ε is maximal on the lines $\omega_1=\omega_2+I^i_{3p}$).

Spatially extended scattering spectrum structure appearing on the line $\omega_1=\omega_2$ corresponds to the *elastic* scattering of a photon by the Ar atom. In this case doubly differential cross section of scattering of a photon by an atom assumes the form

$$\frac{d^2\sigma_\perp}{d\omega_2 d\Omega} = G(\omega_1,\omega_2)\left(\frac{d\sigma_\perp}{d\Omega}\right)_{RS}. \tag{28}$$

In Eq. (28) $(d\sigma_\perp/d\Omega)_{RS}$ is the differential cross section of anomalous elastic scattering of an x-ray photon by the atomic electrons (*RS*: Rayleigh scattering) (Kane *et al.* [45], Pratt [46]). Its analytical structure, absolute values, and profile in the case of anomalous elastic scattering of unpolarized x-ray photon by the Ar atom at scattering angle (i.e., the angle between are wave vectors of the incident and scattered photons) θ=0° (forward scattering) near K, KM_1, and KM_{23} ionization thresholds with inclusion of a wide hierarchy of

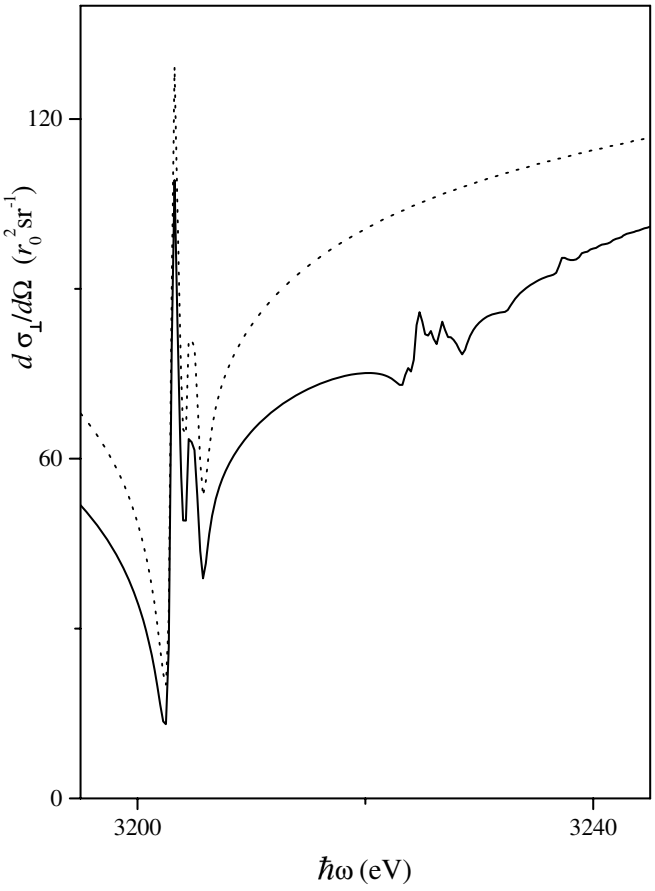

FIG. 2. Differential cross section of anomalous elastic scattering of linearly polarized (perpendicularly to the scattering plane) x-ray photon near K (3206.26 eV, from Ref. [40]) and KM_{23} (3237.40 eV, this work's calculation) ionization thresholds of the free Ar atom. Dashed line–included are the effects of radial relaxation, CL and VC; solid line–included are the effects of radial relaxation, CL, VC and double $1s3p\rightarrow n_1(\varepsilon)l_1n_2(\varepsilon')l_2$ and $1s3s$ $\rightarrow n_1l_1n_2l_2$ excitation/ionization. Scattering angle θ=90°. $\hbar\omega$ is the scattered photon energy, Ω is a solid angle of escaping scattered photon, Γ_{1s}=0.69 eV (from Ref. [34]). Assignment and spectral characteristics of resonances are given in Ref. [47].

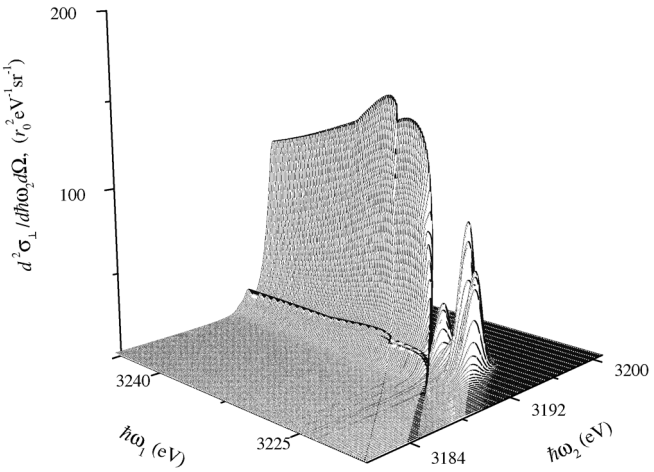

FIG. 3. Doubly differential cross section of resonance inelastic scattering of linearly polarized (perpendicularly to the scattering plane) x-ray photon near KM_{23} (3237.40 eV, this work's calculation) ionization threshold of the free Ar atom. The values of Γ_{1s}, Γ_{beam}, δ_{SO}, and notations are the same as in Fig. 1. Assignment and spectral characteristics of resonances are given in Table I, those of the spatially extended structures of scattering – in Table II.

many-particle effects are studied in detail by Hopersky *et al.* [47].

In this work, in order to give a complete report on the results of the developed many-particle nonrelativistic quantum theory of resonance scattering of photon by an atom, we repeated the calculations of Ref. [47] but for the case of elastic scattering of linearly polarized (perpendicularly to the scattering plane) x-ray photon at $\theta=90°$ for which case there exists the synchrotron experiment by Deslattes *et al.* [1]. Calculations results are presented in Fig. 2.

In the case of the Ar atom, the $\delta_{SO}(3p)=0.179$ eV is small as compared with $\Gamma_{1s}=0.690$ eV which explains the fact that both in the experimental spectra from Ref. [1] and in Fig. 1 (and in the following ones) the spin-doublet components $j+1/2$ and $j-1/2$ $(j=1)$ of the $3p_{1/2,3/2}$ subshell are unresolved.

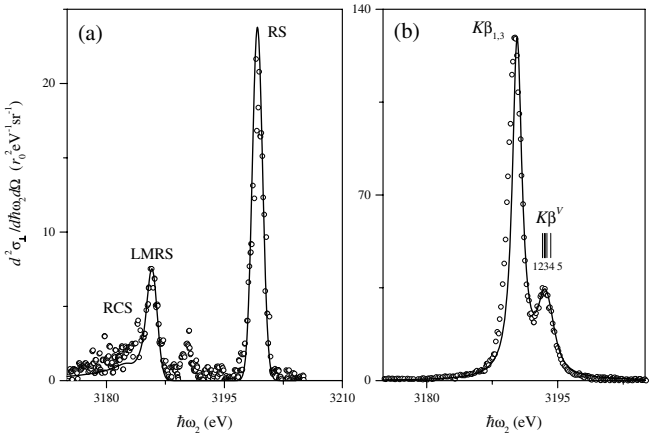

FIG. 4. X-ray $K\beta$ emission spectrum of the free Ar atom at incident photon energies of (a) $\hbar\omega_1=3199.2$ eV and (b) $\hbar\omega_1=3245.9$ eV. Open circles: synchrotron experiment by Deslattes *et al.* [1] (spectrum measured in arbitrary units). The absolute values along the vertical axis are those of the theoretical cross section [see Eqs. (3), (50), and (57)]. Solid line: theory of this work: (a) $\Gamma_{1s}=0.69$ eV (from Ref. [34]), (b) $\Gamma_{1s}=1.29$ eV $(K\beta_{1,3})$, 1.60 eV $(K\beta^V)$ (from Ref. [1]). The values of Γ_{beam}, δ_{SO} and notations are the same as in Fig. 1. The abbreviations RCS, LMRS, and RS are given in the text. The assignment of the resonances in theoretical satellite $K\beta^V$ structure marked with numbers is given in Table II.

B. KM_{23} ionization threshold energy range

In the energy range of the KM_{23} ionization threshold ($I_{1s3p}=3237.40$ eV, this work's calculation) we considered only *double* excitation/ionization effects which are the principal contributors to the integral intensity of multiple excitation/ionization of the Ar atom ground state [1,30,48–55].

Near KM_{23} threshold structure of doubly differential cross section of scattering of x-ray photon by the Ar atom is studied in *two* stages.

At the *first* stage, the states of double excitations [states of Landsberg-Mandelstam-Raman scattering (LMRS)] are considered as intermediate and final ones.

Intermediate states wave functions ($|n\rangle$) and energies (E_n) are obtained in the *LS* coupling scheme in many-configuration Hartree-Fock approximation by diagonalization of the secular equation matrix

$$\langle n|\hat{H}|m\rangle = E_n\delta_{nm}, \tag{29}$$

constructed on a base of the wave functions

$$|n\rangle = \sum_{LS}\sum_{n_{1,2}>f}\sum_{l_{1,2}} a_{12}^{LS}|\zeta n_1 l_1 n_2 l_2(LS);{}^1P_1\rangle, \tag{30}$$

$$\zeta \equiv 1s2s^22p^63s^23p^5({}^{2S+1}P_1), \tag{31}$$

$$n_1 l_1 n_2 l_2 = 4p(s)mp(s), \quad (4s,3d)kd, \quad k=3,4, \quad m=k+1, \tag{32}$$

where a_{12}^{LS} are the configurations mixing coefficients, *LS* is a term of a pair of excited n_1l_1, n_2l_2 electrons, and $\hat{H}$ is a nonrelativistic atomic Hamiltonian.

Radial parts of the n_1l_1, n_2l_2 electrons' wave functions from Eqs. (30) and (32) are obtained by the solution of the Hartree-Fock equations averaged over the terms of the $\zeta n_1 l_1 n_2 l_2$ configuration. Radial parts of the atomic residue electrons' wave functions from Eq. (31) are obtained by the solution of the Hartree-Fock equations averaged over the terms of the configuration ζ.

The wave functions from Eqs. (30)–(32) of the considered states giving the principal contribution to the intensity of double excitation are (listed are only the components with $a_{12}^{LS}\geq 0.4$)

$$|1\rangle = 0.6|\zeta 4p^2({}^3P)\rangle + 0.7|\zeta 4s4d({}^1D)\rangle,$$

$$|2\rangle = -0.6|\zeta 4p^2({}^3P)\rangle + 0.7|\zeta 4s4d({}^1D)\rangle,$$

$$|3\rangle = |\zeta 4p^2[0.6(^1S) + 0.4(^3P)]\rangle - 0.5|\zeta 3d^2(^1S)\rangle,$$

$$|4\rangle = |\zeta 4p^2[0.7(^1D) - 0.4(^1S)]\rangle - 0.4|\zeta 3d^2(^1D)\rangle,$$

$$|5\rangle = |\zeta 4p5p[0.4(^3S) - 0.5(^3D) - 0.6(^3P)]\rangle,$$

$$|6\rangle = 0.8|\zeta 4p5p(^1D)\rangle. \quad (33)$$

The structures of the wave functions from Eq. (33) for $n \leq 4$ demonstrate the significant role of the electrostatic $4p^2-4s4d$, $3d^2$ interaction in the formation of intermediate LMRS states.

Resonance incident photon energies (ω_{1n}; see Table I), as the energies of radiative transitions from the Ar atom ground state to the states from Eq. (33) are calculated with

$$\omega_{1n} = E_n - E(0), \quad (34)$$

where E_n is the energy from Eq. (29) and $E(0)$ is the Hartree-Fock ground state energy of the atom.

Equation (34) does not include the correlation energy, approximately from 1 to 3 eV, for each electron (Nesbet [56], Demekhin *et al.* [57]). This values of neglected correlation energy gives an estimate of the accuracy for radiation transitions energies from Eq. (34).

Final LMRS states wave functions are obtained in one-configuration Hartree-Fock approximation. As final scattering configuration reached by the radiative transitions from intermediate states from Eq. (33), $3p^44p^2(^1S_0, ^1D_2)$is taken for $n \leq 4$, and $3p^44p5p(^1S_0, ^1D_2)$ is taken for $n=5,6$.

We use the approximation in which the energies of all the $|n\rangle \rightarrow |3p^4(4p^2, 4p5p)\rangle$ transitions are the same and equal

$$\omega_0 = \omega_{13} - E(3p^44p^2) + E(0), \quad (35)$$

where $\omega_{13}=3224.4$ eV (see Table I), and E are the averaged over the terms Hartree-Fock energies of respective configurations.

Going outside the frame of the approximation of Eq. (35) is necessary if one is to consider the configurations interaction in scattering final states. This will be the subject of our further studies.

The radial relaxation effect in the Hartree-Fock fields of the deep $1s$ and valence $3p$ vacancy in the construction of the amplitudes of the radiation transitions $[0] \rightarrow |n\rangle$ and $|n\rangle \rightarrow |3p^4(4p^2, 4p5p)\rangle$ is included by the methods of the nonorthogonal orbitals theory. Thus in the case of double $1s3p \rightarrow 4p^2$ excitation of the Ar atom ground state the expression for the radial part of the radiative transition amplitude is ($\hat{D}$ is a many-electron radiation transition operator)

$$\langle 0|\hat{D}|\zeta 4p^2\rangle = M_{sp}\langle 1s_0|\hat{r}|X_1\rangle\langle 3p_0|X_2\rangle, \quad (36)$$

$$M_{sp} = \langle 1s_0|1s\rangle\langle 2s_0|2s\rangle^2\langle 2p_0|2p\rangle^6\langle 3s_0|3s\rangle^2\langle 3p_0|3p\rangle^5, \quad (37)$$

$$|X_1\rangle = |4p\rangle - \sum_{k=2,3} |kp\rangle \frac{\langle kp_0|4p\rangle}{\langle kp_0|kp\rangle}, \quad (38)$$

$$|X_2\rangle = (1-\beta)^{-1/2}\left(|4p\rangle - \sum_{k=2,3} |kp_+\rangle\langle kp_+|4p\rangle\right), \quad (39)$$

$$\beta = \sum_{k=2,3} \langle kp_+|4p\rangle^2. \quad (40)$$

In Eqs. (36)–(40) the radial parts of the l_0, l, and l_+ electron's wave functions are obtained by the solution of term-averaged Hartree-Fock equations for $[0]$, $\zeta 4p^2$ and $1s4p$ configurations, respectively.

Doubly differential LMRS cross section with the participation of double excitation states from Eq. (33), instead of Eq. (3), has the form

$$\frac{d^2\sigma_\perp}{d\omega_2 d\Omega} = r_0^2\left(\frac{\omega_2}{\omega_1}\right)g^{-1}\sum_n D_n L(\omega_1, \omega_{1n})G(\omega_{12}, \omega_{1n} - \omega_0), \quad (41)$$

$$D_n = \frac{\pi}{\gamma_{1s}}[\omega_{1n}(\omega_{1n} - \omega_{12})\langle 0|\hat{D}|n\rangle\alpha_n q]^2, \quad (42)$$

$$q = M\left(\langle 1s|\hat{r}|3p_{++}\rangle - \langle 1s|\hat{r}|2p_{++}\rangle\frac{\langle 2p|3p_{++}\rangle}{\langle 2p|2p_{++}\rangle}\right). \quad (43)$$

In Eqs. (42) and (43) the radial parts of the l and l_{++} electrons' wave functions are obtained by the solution of term-averaged Hartree-Fock equations for configurations $3p^4(4p^2, 4p5p)$ and $\zeta(4p^2, 4p5p)$, respectively, α_n is a resulting angular parts coefficient of the transition, q is the radial part of the amplitude of radiative $|n\rangle \rightarrow |3p^4(4p^2, 4p5p)\rangle$ transition, and M is the product of the overlap integrals of the wave functions of the electrons not involved in the transition.

Calculated cross section from Eq. (41) near KM_{23} ionization threshold of the Ar atom are presented in Table I and in Fig. 3.

At the *second* stage, the states of excitation/ionization ($n=4,5$)

$$\omega_1 + [0] \rightarrow (K_{1n})\varepsilon p(^1P_1) \rightarrow (K_{2n})\varepsilon p(^1S_0, ^1D_2) + \omega_2, \quad (44)$$

and the states of double ionization

$$\omega_1 + [0] \rightarrow \zeta\varepsilon p\varepsilon' p(^1P_1) \rightarrow 3p^4\varepsilon p\varepsilon' p(^1S_0, ^1D_2) + \omega_2 \quad (45)$$

[states of the resonant Compton scattering (RCS)] are taken as intermediate and final states of scattering. In Eq. (44) $K_{1n} \equiv \zeta np$ and $K_{2n} \equiv 3p^4np$ are the atomic residues with an excited np electron.

The channels of excitation/ionization of the Ar atom ground state $1s3p \rightarrow np\varepsilon p$ are opened at ω_1 $(eV)=3228.5$ $(n=4)$; 3232.4 $(n=5)$ (this work's calculation).

Total wave functions and energies of intermediate and final scattering states from Eq. (44) are obtained in the *LS* coupling scheme in one-configuration Hartree-Fock approximation by diagonalization of secular equations matrices. The secular equations are built on the bases of the wave functions

$|\zeta(T_1)np(T_2)\rangle$ and $|3p^4(T_3)np(T_4)\rangle$, respectively. Here T_2 and T_4 are the resulting terms of the atomic residues $\zeta(T_1)$and $3p^4(T_3)$, and of the excited $np(^2P)$ electron.

When calculating the multiplet structure of $\zeta\varepsilon p\varepsilon' p$ and $3p^4\varepsilon p\varepsilon' p$ states of scattering with two εp and $\varepsilon' p$ electrons of the continuous spectrum from Eq. (45) we neglected $1s-\varepsilon p$ and $3p-\varepsilon p$ interaction by taking the electrostatic integrals $F_2(3p\varepsilon p)=G_{0,2}(3p\varepsilon p)=G_1(1s\varepsilon p)=0$.

Diagonalization of the secular equations' matrices give the following results.

(1) Among the components of the K_{1n} multiplet of intermediate states, only $^1P^2S$ and $^3P^2P$ terms of the configuration K_{14} are mixed

$$\psi_1 = 0.97(^1P,^2S) - 0.24(^3P,^2P),$$

$$\psi_3 = 0.24(^1P,^2S) + 0.97(^3P,^2P), \tag{46}$$

and $^1P^2S$ and $^3P^2S$ terms of the configuration K_{15} are mixed

$$\phi_1 = 0.95(^1P,^2S) - 0.30(^3P,^2S),$$

$$\phi_3 = 0.30(^1P,^2S) + 0.95(^3P,^2S), \tag{47}$$

where $(T_1,T_2)\equiv|\zeta(T_1)np(T_2)\rangle$, $n=4,5$.

(2) Among the components of the K_{2n} multiplet of final states, only $^3P^2P$ and $^1D^2P$ terms of the configuration K_{24} are mixed

$$\varphi_1 = 0.34(^3P,^2P) + 0.94(^1D,^2P),$$

$$\varphi_3 = 0.94(^3P,^2P) - 0.34(^1D,^2P), \tag{48}$$

where $(T_3,T_4)\equiv|3p^4(T_3)4p(T_4)\rangle$.

Emission photons energies are calculated with the formula

$$\omega_{in} = E(K_{1n}) - E(K_{2n}) + E_i(K_{1n}) - E_i(K_{2n}) + \omega_{1s}^{rel.}, \tag{49}$$

where E is the term-average Hartree-Fock energies of the K_{1n} and K_{2n} states, E_i are the energies of the $i\equiv(T_1,T_2)$, (T_3,T_4) terms of multiplets components [including the transitions with the participation of the states from Eqs. (46)–(48)] with respect to their centers of gravity, $\omega_{1s}^{rel.}=10$ eV is the relativistic correction to the Hartree-Fock energy of the Ar K level (theoretical result by Kuchas *et al.* [58]).

Doubly differential RCS cross section with the participation of excitation/ionization states, instead of Eq. (3), has the form $(n=4,5)$

$$\frac{d^2\sigma_\perp^{(n)}}{d\omega_2 d\Omega} = r_0^2\left(\frac{\omega_2}{\omega_1}\right)g^{-1}S_n\sum_i D_{ni}L(\omega_2,\omega_{in}), \tag{50}$$

$$S_n = \frac{1}{2} + \frac{1}{\pi}\arctan\left(\frac{\omega_{12} - E(K_{2n}) + E(0)}{\gamma_{1s}}\right), \tag{51}$$

$$D_{ni} = \frac{\pi}{\gamma_{1s}}[\omega_{in}(\omega_{12}+\omega_{in})A_{in}]^2, \tag{52}$$

$$A_{in} = N(\alpha_{in}B_{\varepsilon n} + \beta_{in}B_{n\varepsilon})\langle 1s|\hat{r}|\overline{3p}\rangle, \tag{53}$$

$$B_{\varepsilon n} = \langle 3p_0|\overline{\varepsilon p}\rangle d_n, \tag{54}$$

$$|\overline{3p}\rangle = |3p_+\rangle - |2p_+\rangle\frac{\langle 2p_0|3p_+\rangle}{\langle 2p_0|2p_+\rangle}, \tag{55}$$

$$d_n = \langle 1s_0|\hat{r}|np_+\rangle - \sum_{k=2,3}\langle 1s_0|\hat{r}|kp_+\rangle\frac{\langle kp_0|np_+\rangle}{\langle kp_0|kp_+\rangle}. \tag{56}$$

Here ω_{in} is determined in Eq. (49), α_{in} and β_{in} are the resulting angular coefficients of the transitions, N is the product of the overlap integrals of the wave functions of the electrons not involved in the transition. Radial parts of the l_0, l_+, and l electron's wave functions are obtained by solving the term-averaged Hartree-Fock equations for [0], K_{1n} and K_{2n} configurations, respectively.

Doubly differential RCS cross section with the participation of double ionization states, instead of Eq. (3), has the form

$$\frac{d^2\sigma_\perp}{d\omega_2 d\Omega} = r_0^2\left(\frac{\omega_2}{\omega_1}\right)g^{-1}S\sum_i D_i L(\omega_2,\omega_i), \tag{57}$$

$$D_i = \frac{\pi}{\gamma_{1s}}[\omega_i(\omega_{12}+\omega_i)]^2\int_0^a A_i^2(x,\omega_1)dx, \tag{58}$$

where the upper integration limit $a=\omega_1+I_{1s3p}-\omega_{1s}^{rel.}$, ω_i is like ω_{in} in Eq. (49) and S is like S_n in Eq. (51) with $n\to\varepsilon=0$, A_i in Eq. (58) is like A_{in} in Eqs. (52)–(56) with $\varepsilon\to x$ and $n\to a-x$.

Calculated cross sections from Eqs. (50) and (57) near Ar KM_{23} ionization threshold are presented in Table II and in Figs. 3 and 4(b).

C. Comparison of theory with experiment

This work's calculations results are compared with the results of the synchrotron experiment by Deslattes *et al.* [1] in Fig. 4.

The experiment is performed for the scattering angle of $\theta=90°$ and the x-ray $K\beta$ emission spectrum of the free Ar atom is measured at incident photon energies of ω_1(eV) =3199.2, 3213.1, 3245.9, and 3281.4 for emission photon energies ω_2 from 3175 to 3205 eV.

In this work we compare our results with the experiment only at ω_1(eV)=3199.2 [see Fig. 4(a)], 3213.1 and 3245.9 [see Fig. 4(b)].

Comparison with the experiment at $\omega_1=3213.1$ eV is not presented with a separate figure. The reason is that at this incident photon energy, the experiment reveals only the $K\beta_{1,3}$ resonance of the emission spectrum at $\omega_2=3190$ eV. The profile and the intensity of this resonance are well reproduced by our calculation with the experimental values from Ref. [1] of the width $\Gamma_{1s}=1.29$ eV and parameter $\Gamma_{beam}=1.30$ eV and the absolute value of the cross section at the resonance maximum of 137.32 (r_0^2 eV^{-1} sr^{-1}). At that, together with the $K\beta_{1,3}$ resonance of the emission spectrum, our theory predicts the appearance, at $\omega_1=\omega_2$, of the resonance in doubly differential cross section of anomalous *elastic* scattering with the absolute value at the resonance maximum of 43.48 (r_0^2eV^{-1} sr^{-1}).

At $\omega_1=3281.4$ eV, in the experimental Ar$K\beta$ emission spectrum, there appears a well defined extended β'' satellite at ω_2 from 3195 to 3200 eV. Theoretical assignment of this satellite deals with the inclusion, in the first place (see, for example, Dyall and La Villa [48]), of double $1s3s \rightarrow nln'(\varepsilon)l$ and triple $1s3p3p \rightarrow 4p^2n(\varepsilon)l$ excitation/ionization processes in the Ar atom ground state. We did not include these processes in this work.

Experimental Ar $K\beta$ emission spectrum is obtained in arbitrary units for intensity. Because of that, we "tied" its profile to the theoretical values of the cross section from Eq. (3) at the maximum of the riblike structure of $1s \rightarrow 4p$ LMRS resonance 7.54 (r_0^2 eV^{-1} sr^{-1}) at $\omega_2=3185.9$ eV [see Fig. 4(a)], and to the theoretical values of the sum of cross sections (50) and (57) at the maximum of the intense $K\beta^V$ satellite emission spectrum 34.93 (r_0^2 eV^{-1} sr^{-1}) at $\omega_2=3193.6$ eV [see Fig. 4(b)].

Theoretical scattering cross section in Fig. 4(a) is obtained with inclusion of a wide hierarchy of many-particle effects (see Sec. II).

Inclusion of CL and VC effects increases by ~25% the absolute values of the cross section from Eq. (3) in the region of the formation of the RCS profile and LMRS resonance at ω_2 from 3175 to 3188 eV calculated considering only the effect of radial relaxation of intermediate scattering states in the field of the deep $1s$ vacancy.

Inclusion of *shake–up* (*off*) processes near the KM_{23} ionization threshold decreases by ~16% the absolute value of the RS resonance maximum at $\omega_2=\omega_1=3199.2$ eV calculated with inclusion of only CL,VC, and radial relaxation effects. Indeed, Fig. 2 shows that the inclusion of the transitions into the states of double excitation from Eq. (33), excitation/ionization $(K_{1n})\varepsilon p$ from Eq. (44) and double ionization $\zeta\varepsilon p\varepsilon' p$ from Eq. (45) leads to redistribution of the anomalous elastic scattering intensity from the regions of K and KM_{23} ionization thresholds to higher and lower energy regions of the scattering spectrum.

Theoretical cross section in Fig. 4(b) is obtained with inclusion of only radial relaxation, multiplet splitting, excitation/ionization, and double ionization effects. The role of CL and VC effects in the incident photon energy region $\omega_1 \sim 3240$ eV $> I_{1s}$ becomes insignificant (~3%) and they was not included.

The contribution from the *contact* part of doubly differential cross section of inelastic scattering at incident photon energies ω_1 from 3200 to 3250 eV makes a small value of about 10^{-5} (r_0^2 eV^{-1} sr^{-1}) and was not considered. However, from the methodological point of view, we note the following. In the case of the Ar atom it is already at $\omega_1 \geq 1600$ eV and the valence $3p$ shell mean radius of $r_{3p}=0.88$ Å that the condition of applicability of the *dipole* approximation for the *contact transition operator* is not fulfilled. Indeed, instead of the condition $qr \rightarrow 0$ (q is the module of the momentum transferred to an atom [7]), at scattering angle $\theta=90°$ one has $qr \geq 1$. For this reason, one has to employ the formulas for the amplitudes of contact inelastic scattering derived by Hopersky *et al.* [25] *outside* the frame of the dipole approximation.

One can see that this work's theory compares with the experiment well.

The emission spectrum structure seen in the experiment at $\omega_1=3199.2$ eV for ω_2 from 3188 to 3200 eV (energy region of formation of principal $K\beta_{1,3}$ and satellite $K\beta^V$ and $K\beta''$ structures) [see Fig. 4(a)] has not been assigned. The authors of Ref. [1] argued that this structure is generated by *higher* harmonics present in the monochromatized incident x-ray radiation. Theoretical study of this statement is outside the frame of our work.

IV. CONCLUSION

We performed the first theoretical study of the influence of a wide hierarchy of many-particle effects on the absolute values and the extended-in-space profile of doubly differential cross section of resonance scattering of an x-ray photon by a *free* atom near the ionization threshold of its inner shell. The Ar atom was chosen as an object (energy region of K and KM_{23} ionization thresholds).

Our study established the following.

The effect of radial relaxation of intermediate scattering states' electron shells in the self-consistent Hartree-Fock field of the deep $1s$ vacancy decreases practically by a factor of 2 the theoretical absolute values of the inelastic scattering cross sections at energies of the $K\beta_{1,3}$ emission spectrum formation in the free Ar atom as compared with those calculated without this effect. At that, the effects of correlation loosening and vacuum correlations determine substantially the absolute values and the spatially extended shape of the inelastic scattering cross section, in the first place, in the region of the leading resonances of Landsberg-Mandelstam-Raman scattering and resonance Compton scattering.

The processes of double excitation/ionization of the atomic ground state, the radial relaxation and multiplet splitting effects in intermediate and final scattering states determine substantially the absolute values and the spatially extended shape of the fine structure of inelastic scattering cross section at energies of the $K\beta^V$ satellite structure formation in $K\beta$ emission spectrum of the free Ar atom.

One may suppose that the above conclusions are valid also in the case of the theoretical description of double differential cross section of resonance scattering of an x-ray photon near the ionization thresholds of the deep $2s$ and $2p$ shells of the Ar atom. Near Ar L_1 and Ar M_1 ionization thresholds one must expect the increase of the role of the effect of intershell correlations (Hopersky and Yavna [59,60]).

ACKNOWLEDGMENT

We thank Professor Dr. A. G. Kochur for helpful discussions.

[1] R. D. Deslattes, R. E. La Villa, P. L. Cowan, and A. Henins, Phys. Rev. A **27**, 923 (1983).
[2] J. Tulkki, Phys. Rev. A **27**, 3375 (1983).
[3] G. S. Landsberg and L. I. Mandelstam, Z. Phys. **50**, 769 (1928).
[4] C. V. Raman, Indian J. Phys. **2**, 387 (1928).
[5] A. H. Compton, Phys. Rev. **21**, 483 (1923).
[6] T. Åberg and J. Tulkki, in *Atomic Inner-Shell Physics*, edited by B. Crasemann (Plenum Press, New York, 1985), Chapter 10, pp. 419–463.
[7] P. P. Kane, Phys. Rep. **218**, 67 (1992).
[8] P. A. Raboud, M. Berset, J.-Cl. Dousse, Y. P. Maillard, O. Mauron, J. Hoszowska, M. Polasik, and J. Rzadkiewicz, Phys. Rev. A **65**, 062503 (2002).
[9] H. Czerwinski, F. Smend, D. Shaupp, M. Schumacher, A. H. Millhouse, and H. Schenk–Strauss, Z. Phys. A **322**, 183 (1985).
[10] M. A. MacDonald, S. H. Southworth, J. C. Levin, A. Henins, R. D. Deslattes, T. LeBrun, Y. Azuma, P. L. Cowan, and B. A. Karlin, Phys. Rev. A **51**, 3598 (1995).
[11] M. A. Kornberg, A. L. Godunov, S. Itza–Ortiz, D. L. Ederer, J. H. McGuire, and L. Young, J. Synchrotron Radiat. **9**, 655 (2002).
[12] H. Daido, Rep. Prog. Phys. **65**, 298 (2002).
[13] J. Lindl, Phys. Plasmas **2**, 3933 (1995).
[14] M. Miceli, A. Decourchelle, J. Ballet, F. Bocchino, J. P. Hughes, U. Hwang, and R. Petre, Astron. Astrophys. **453**, 567 (2006).
[15] F. Gel'mukhanov and H. Ågren, Phys. Rep. **312**, 87 (1999).
[16] A. Kotani and S. Shin, Rev. Mod. Phys. **73**, 203 (2001).
[17] R. D. Deslattes, E. G. Kessler Jr., P. Indelicato, L. de Billy, E. Lindroth, and J. Anton, Rev. Mod. Phys. **75**, 35 (2003).
[18] A. P. Jucys, E. P. Našlėnas, and P. S. Žvirblis, Int. J. Quantum Chem. **6**, 465 (1972).
[19] von L. Zülicke, *Quantenchemie. Band 1. Grundlagen und Allgemeine Methoden* (Berlin: VEB Deutscher Verlag der Wissenschaften, 1973).
[20] V. L. Sukhorukov, V. Ph. Demekhin, V. A. Yavna, A. I. Dudenko, and V. V. Timoshevskaya, Opt. Spektrosk. **55**, 229 (1983) [Opt. Spectrosc. **55**, 135 (1983)].
[21] M. Reed and B. Simon, *Methods of Modern Mathematical Physics. V. 1. Functional Analysis* (Academic Press, New York, 1972).
[22] V. L. Sukhorukov, V. Ph. Demekhin, V. V. Timoshevskaya, and S. V. Lavrentiev, Opt. Spektrosk. **47**, 407 (1979) [Opt. Spectrosc. **47**, 228 (1979)].
[23] M. Ya. Amusia, *Atomic Photoeffect* (Plenum Press, New York, 1990).
[24] V. Schmidt, Rep. Prog. Phys. **55**, 1483 (1992).
[25] A. N. Hopersky, A. M. Nadolinsky, and V. A. Yavna, Zh. Eksp. Teor. Fiz. **128**, 698 (2005) [JETP **101**, 597 (2005)].
[26] A. N. Hopersky, Opt. Spektrosk. **85**, 377 (1998) [Opt. Spectrosc. **85**, 346 (1998)].
[27] A. N. Hopersky, Radiat. Phys. Chem. **64**, 169 (2002).
[28] A. N. Hopersky and V. V. Chuvenkov, J. Phys. B **36**, 2987 (2003).
[29] A. N. Hopersky and V. A. Yavna, Zh. Eksp. Teor. Fiz. **108**, 1223 (1995) [JETP **81**, 671 (1995)].
[30] V. L. Sukhorukov, A. N. Hopersky, I. D. Petrov, V. A. Yavna, and V. Ph. Demekhin, J. Phys. (Paris), Colloq. **48**, 1677 (1987).
[31] A. P. Jucys, Adv. Chem. Phys. **14**, 131 (1969).
[32] Ch. Froese–Fischer, *The Hartree-Fock Method for Atoms* (New York: John Wiley, 1977).
[33] N. A. Kulagin and I. I. Zalyubovski, J. Phys. B **14**, 1537 (1981).
[34] D. V. Morgan, R. J. Bartlett, and M. Sagurton, Phys. Rev. A **51**, 2939 (1995).
[35] T. Kylli, J. Karvonen, H. Aksela, A. Kivimäki, S. Aksela, R. Camilloni, L. Avaldi, M. Coreno, M. de Simone, R. Richter, K. C. Prince, and S. Stranges, Phys. Rev. A **59**, 4071 (1999).
[36] T. W. Gorczyca and F. Robicheaux, Phys. Rev. A **60**, 1216 (1999).
[37] S. Lauer, H. Liebel, F. Vollweiler, H. Schmoranzer, B. M. Lagutin, Ph. V. Demekhin, I. D. Petrov, and V. L. Sukhorukov, J. Phys. B **32**, 2015 (1999).
[38] H. Katori and F. Shimizu, Phys. Rev. Lett. **70**, 3545 (1993).
[39] K.-N. Huang, M. Aoyagi, M. H. Chen, B. Crasemann, and H. Mark, At. Data Nucl. Data Tables **18**, 243 (1976).
[40] M. Breinig, M. H. Chen, G. E. Ice, F. Parente, and B. Crasemann, Phys. Rev. A **22**, 520 (1980).
[41] P. Glans, R. E. La Villa, M. Ohno, S. Svensson, G. Bray, N. Wassdahl, and J. Nordgren, Phys. Rev. A **47**, 1539 (1993).
[42] R. I. Karazija, *Introduction to the Theory of X-Ray and Electronic Spectra of Free Atoms* (Plenum Publishing Corporation, New York, 1992).
[43] A. N. Hopersky, V. A. Yavna, A. M. Nadolinsky, and D. V. Dzuba, J. Phys. B **37**, 2511 (2004).
[44] A. N. Hopersky, A. M. Nadolinsky, D. V. Dzuba, and V. A. Yavna, J. Phys. B **38**, 1507 (2005).
[45] P. P. Kane, L. Kissel, R. H. Pratt, and S. C. Roy, Phys. Rep. **140**, 75 (1986).
[46] R. H. Pratt, Radiat. Phys. Chem. **74**, 411 (2005).
[47] A. N. Hopersky, V. A. Yavna, and V. A. Popov, J. Phys. B **29**, 461 (1996).
[48] K. G. Dyall and R. E. La Villa, Phys. Rev. A **34**, 5123 (1986).
[49] J. W. Cooper, Phys. Rev. A **38**, 3417 (1988).
[50] H. P. Saha, Phys. Rev. A **42**, 6507 (1990).
[51] M. Deutsch, N. Maskil, and W. Drube, Phys. Rev. A **46**, 3963 (1992).
[52] T. Hayaishi, E. Murakami, Y. Morioka, H. Aksela, S. Aksela, E. Shigemasa, and A. Yagishita, J. Phys. B **25**, 4119 (1992).
[53] M. Štuhec, A. Kodre, M. Hribar, D. Glavič-Cindro, I. Arčon, and W. Drube, Phys. Rev. A **49**, 3104 (1994).
[54] L. Avaldi, R. Camilloni, G. Stefani, C. Comicioli, M. Zacchigna, K. C. Prince, M. Zitnik, C. Quaresima, C. Ottaviani, C. Crotti, and P. Perfetti, J. Phys. B **29**, L737 (1996).
[55] J. Padežnik Gomilšek, A. Kodre, I. Arčon, and Rok Prešeren, Phys. Rev. A **64**, 022508 (2001).
[56] R. K. Nesbet, Phys. Rev. **175**, 2 (1968).
[57] V. Ph. Demekhin, Ph. V. Demekhin, A. G. Kochur, and N. V. Demekhina, Zh. Strukt. Khim. **39**, 1001 (1998), in Russian.
[58] S. A. Kuchas, A. V. Karosene, and R. I. Karazija, Lith. J. Phys. 13, 593 (1978).
[59] A. N. Hopersky and V. A. Yavna, Opt. Spektrosk. **82**, 5 (1997) [Opt. Spectrosc. **82**, 1 (1997)].
[60] A. N. Hopersky and V. A. Yavna, Opt. Spektrosk. **85**, 904 (1998) [Opt. Spectrosc. **85**, 826 (1998)].